HPLC and mass spectrometry analysis of dolichol-phosphates at the cell culture scale

Micha A. Haeuptle[1], Andreas J. Hülsmeier[1] and Thierry Hennet[1]

[1]Institute of Physiology, University of Zürich, Winterthurerstrasse 190, CH-8057 Zürich, Switzerland

Corresponding author: Thierry Hennet
Institute of Physiology
Winterthurerstrasse 190
CH-8057 Zürich
Switzerland
Phone: +41 44 635 50 80
Fax: +41 44 635 68 14
E-mail: thennet@access.uzh.ch

Subject category: Regular article

Running title: Dolichol-phosphate analysis

Abstract

Dolichols (Dol) are polyprenol lipids that are essential structural components of eukaryotic membranes. In addition, the phosphorylated derivatives of Dol function as lipid anchor of mono- and oligosaccharide precursors involved in protein glycosylation. The biological importance of Dol-phosphates (Dol-P) is illustrated by the severe outcome of human disorders linked to Dol biosynthetic defects, such as Dol-kinase deficiency. For characterization of inherited human diseases and evaluation of therapeutic trials, cultured cells often serve as a sole possible source for experimentation. Limited amounts of cell culture material render the quantitative analysis of Dol a challenging task. Here, we present HPLC and mass spectrometry based approaches to analyse and quantitate Dol-P from cultured human cells. The composition of naturally occurring Dol-P and the saturation state of the α-isoprene units was identified by negative ion electrospray ionization mass spectrometry. Furthermore, fluorescently labelled Dol-P were separated by HPLC and quantified by comparison to known amounts of the internal standard polyprenol-P. The effect of pravastatin, a 3-hydroxy-3-methyl-glutaryl coenzyme-A reductase inhibitor, on the formation of Dol-P in HeLa cells was investigated. As expected, this treatment led to a decrease of Dol-P down to 35% of normal levels.

Keywords

Dolichol-phosphate, mass spectrometry, HPLC, cholesterol pathway, statin, glycosylation

Introductory statement

Dolichols (Dol) are essential components of eukaryotic membranes, where they contribute to the organisation and fluidity of the lipid bilayer and enhance vesicle fusion [1]. Their composition varies between the kingdoms of life in respect to the number of isoprene subunits, although all Dol are assembled in the identical *trans*-*trans*-poly*cis* conformation. In contrast to prokaryotic polyprenols, Dol α-isoprene residues are saturated [2]. Starting from acetate, the pathway leading to the formation of Dol leads via mevalonate to farnesyl-pyrophosphate and is up to this point identical to the cholesterol and ubiquinone biosynthesis pathway [1]. The enzyme *cis*-prenyltransferase catalyzes the elongation of farnesyl-pyrophosphate by sequential condensation of isopentenyl-pyrophosphate [2]. Prior to the NADPH-dependent reduction of the α-isoprene unit, the entirely unsaturated polyprenol-pyrophosphate intermediates are dephosphorylated by mono- or pyrophosphate phosphatases. In a terminatory step, the resulting Dol are phosphorylated by the CTP-dependent Dol-kinase [3].

Dolichol-phosphates (Dol-P) serve as lipid carriers of mono- and oligosaccharides involved in several protein glycosylation pathways [4; 5] and in the formation of the glycosylphosphatidylinositol anchor [6]. Pathogenic alterations of Dol and Dol-P levels and composition have been observed in the context of liver cancer [7], Alzheimer's disease [8], ceroid lipofuscinosis [9] and Dol-kinase deficiency [10].

To date, only few techniques have been described for the analysis and quantification of Dol-P [11; 12; 13]. HPLC-based methods separate radio-labelled or fluorescently tagged polyprenol-P and are mainly restricted to tissue-derived samples [14; 15]. Whereas several mass spectrometry (MS) methods for the analysis of free Dol have been described [16; 17; 18; 19; 20; 21], no MS method has been established to analyse Dol-P from mammalian sources, despite the essential role of Dol-P in protein glycosylation [4]. Solely, Griffiths and co-workers have configured their MS setup to such an extent that it

enabled the detection of Dol-sulphates and Dol-P from standard mixtures [18]. Furthermore, desorption electron impact and desorption chemical ionization MS spectra of mycobacterial decaprenyl-P have been recorded [22].

The recent discovery of inherited human disorders of Dol-P and Dol-P linked oligosaccharide biosynthesis [10; 23; 24] calls for an accurate and quantitative method to measure variations of Dol-P levels in minute amounts. Here, we present the first detailed analysis of Dol-P at the cell culture scale by electrospray ionization MS (ESI-MS), which enabled the determination of Dol-P composition as well as the saturation state of the α-isoprene units. In addition, a HPLC method was adapted to allow the quantitative analysis of Dol-P isolated from cell cultures.

Materials and Methods

Materials

C_{80}-polyprenol-P and C_{95}-Dol-P standards were purchased from Larodan Fine Chemicals (Sweden). The mixed Dol-P standard and the fluorophore 9-anthryldiazomethane (9-ADM) were from Sigma-Aldrich (Switzerland). Acetonitrile (Scharlau, Spain), dichloromethane (Sigma-Aldrich) and *n*-hexane (Scharlau) were at least of HPLC grade. Residual reagents were of analytical grade.

Cell culture

HeLa cells were cultured in DMEM (Invitrogen, USA) supplemented with 10% fetal calf serum (Bioconcept, Switzerland) under 5% CO_2 at 37°C. During statin treatment, the cells were grown for 72 hours in medium containing 50 µM pravastatin (Calbiochem, USA) and the medium was changed every 24 hours.

Extraction, hydrolysis and purification of Dol and Dol-P

The extraction protocol of Elmberger and coworkers set up for tissue samples [12] was adapted for cultured cells. Approximately 3 x 10^8 HeLa cells were released by trypsinization, washed once with medium and resuspended in 6 ml H_2O. Prior to the addition of 6 ml MeOH to the sample, 25 µg of C_{80}-polyprenol-P were added as internal standard. Alkaline hydrolysis and subsequent partitioning were performed as described [12]. Briefly, the cell suspension was hydrolyzed by addition of 3 ml 15 M KOH and heated at 100°C for 60 min. After partitioning by addition of 6 ml MeOH and 24 ml dichloromethane, residual Dol-ester were further hydrolyzed at 40°C for 60 min. The lower phase was washed five times with Folch upper phase (dicholomethane / MeOH / H_2O; 3:48:47) and evaporated to dryness.

Purification and separation of Dol and Dol-P were accomplished according to Elmberger *et al* [12]. Briefly, Dol and Dol-P were purified on a C_{18} Sep Pak column (Waters, USA) followed by their separation on a Silica Sep Pak column (Waters).

Dimethylation and selective demethylation of Dol-P

Dol-P were dissolved in 3 ml diethylether and given to the outside tube of an Aldrich diazomethane generator system (Sigma-Aldrich). In the inside tube, 0.35 g diazald (Sigma-Aldrich) were suspended in 1 ml carbitol (Sigma-Aldrich). After assembly of the two parts and cooling in an ice bath, 1.5 ml 37% KOH were added dropwise to the inner tube. The resulting excess of diazomethane could be observed as yellow staining of the diethylether phase. After an incubation of 60 min on ice, the inside tube was removed and dimethylation of Dol-P was continued in the outside tube at room temperature for 2 h. The reaction was stopped by evaporation of the diethylether under a stream of nitrogen. The reaction products were dissolved in 4 ml of *tert*-butylamine (Sigma-Aldrich) and incubated for 14 h at 70°C to attain selective demethylation of dimethylated Dol-P [15]. After evaporation of the *tert*-butylamine, monomethylated Dol-P were acidified by addition of 1.5 ml of 0.1 *N* HCl, subsequently extracted three times with 3 ml of diethylether and evaporated to complete dryness.

9-ADM labelling

Monomethylated or untreated Dol-P were labelled with the fluorophore 9-ADM according to the protocol of Yamada and coworkers [15]. Briefly, the sample was dissolved in 600 µl of diethylether saturated with 9-ADM and incubated for 6 h on ice in the dark. The reaction was stopped by evaporation of the diethylether, and unreacted 9-

ADM was separated from the reaction products by organic extraction [15]. Labelled Dol-P were dissolved in 100 µl of acetonitrile/dichloromethane (3:2).

HPLC

Chromatographic separation was performed using a LaChrom D-7000 HPLC system (Merck, Germany) equipped with an Inertsil ODS-3 column (5 µm, 4.6 x 250 mm; GL Sciences Inc., Japan) including a pre-column and a LaChrom L-7485 fluorescence detector. Isocratic elution in acetonitrile/dichloromethane (3:2) containing 0.01% diethylamine (Sigma-Aldrich) was carried out at a flow rate of 1 ml/min at 30°C [15]. Fluorescence was detected by excitation at 365 nm and emission at 412 nm.

Mass spectrometry

Negative ion mass spectrometry was performed on a 3200 QTRAP mass spectrometer equipped with a nanoelectrospray ion source (NanoSpray II; Applied Biosystems, USA) and an Eksigent NanoLC-2D system (Eksigent Technologies, USA). Samples were dissolved in dissolution solvent (90% acetonitrile, 10% *n*-hexane, 0.01% diethylamine) and directly injected into a 10 µl injection loop. After loading, the loop was switched in line a 20 µm ID, fused silica capillary, connected to the emitter tip of the nanoelectrospray ion source. The sample was introduced to the ion source using the dissolution solvent at a flow rate of 0.4 µl/min. All mass spectra were acquired manually in ion trapping modes and for the Enhanced MS scans the following settings were applied: Curtain Gas flow: 10 psi, collision gas pressure: high, ion spray voltage: between -2400 V and -4500 V, interface heater temperature: 150°C, declustering potential: -200 V, entrance potential: -10 V, collision energy -10 V. Negative ion fragment spectra were acquired in Enhanced Product Ion mode and the collision energy was set to -100 V.

Results

The detection of Dol-P by direct infusion negative ion nano electronspray MS was first demonstrated of C_{95}-Dol-P standards ($C_{95}H_{156}PO_4^-$; ω-t_2-c_{15}-S-P). C_{95}-Dol-P could be monitored at m/z 1392.5 (Fig. 1A), which is consistent with the theoretical mass of 1392.17 Da. The commercially available standards also contained small amounts of C_{90}-Dol-P ($C_{90}H_{148}PO_4^-$; 1324.11 Da) and C_{100}-Dol-P ($C_{100}H_{164}PO_4^-$; 1460.24 Da), which could be observed at m/z 1324.4 and 1460.6, respectively (Fig. 1A). To confirm the identity of the C_{95}-Dol-P, the species at m/z 1392.5 was subjected to collision induced fragmentation. The resulting MS/MS spectrum (Fig. 1B) showed a major fragment series starting at m/z 164.9 (Table 1). The 164.9 Da fragment ion was assigned to reduced monoprenyl-P $C_5H_{10}PO_4^-$ (Fig. 1B insert) featuring a mass of 165.03 Da. Additional minor fragment series were also observed in the MS/MS spectrum with the starting ions at m/z 122.8 and 178.9, respectively (Fig. 1B). All three decay series depicted the sequential elimination of single isoprene (C_5H_8; 68.06 Da) units [21] (Table 1), thereby validating the assignments of the polyprenol C_{95}-Dol-P standard.

The saturated C_{80}-polyprenol-P standard ($C_{80}H_{130}PO_4^-$; ω-t_2-c_{13}-P) was also analyzed by ESI-MS. The resulting spectrum showed a main peak at m/z 1186.7, which corresponded to hexadecaprenyl-P with the theoretical mass of 1185.97 Da (Fig. 1C). The signals at m/z 1202.6 and 1218.4 differed from the main signal by 16 Da increments, which corresponded to oxidized forms of the C_{80}-polyprenol-P. The spectrum showed that the standard was not completely monomolecular, since traces of C_{75}-polyprenol-P ($C_{75}H_{122}PO_4$-; 1117.91 Da) were recorded at m/z 1120.2 (Fig. 1C). Fragmentation of the C_{80}-polyprenol-P yielded a similar decay series (Fig. 1D) as observed for the C_{95}-Dol-P (Fig. 1B), thereby confirming its polymeric isoprene composition. As expected, the entire

fragment ion series starting at m/z 162.7 ($C_5H_8PO_4^-$, 163.02 Da calculated, Fig. 1D) was shifted by 2 Da due to the saturated α-isoprene unit of the C_{80}-polyprenol-P (Table 2). In a second approach, the C_{95}-Dol-P standards was labelled with 9-ADM without prior treatment. The purified products (Fig. 2C, insert) were separated isocratically by HPLC. The resulting fluorescent profile showed the elution of 9-ADM labelled C_{95}-Dol-P as a sharp peak at a retention time of 65.1 min (Fig. 2A). Notably, two additional fluorescent species were observed eluting at 52.8 min and 80.7 min. Considering the ESI-MS spectrum of unlabelled C_{95}-Dol-P standards (Fig. 1A), these peaks likely represented 9-ADM labelled C_{90}- and C_{100}-Dol-P. The ESI-MS analysis of the collected main peak confirmed the expected composition of the product with an m/z of 1582.5 ($C_{110}H_{166}PO_4^-$; 1582.25 Da calculated), while only traces of unlabelled standards could be detected at m/z 1392.7 (Fig. 2C). The C_{80}-polyprenol-P standard was used as spiking compound to quantify the levels of Dol-P in cell culture samples. The analysis of 2 µg of 9-ADM labelled C_{80}-polyprenol-P (Fig. 2D, insert) by HPLC yielded a peak eluting at a retention time of 31.6 min (Fig. 2B). The identity of this peak was confirmed by ESI-MS recording (Fig. 2D), which produced the expected ion at m/z 1376.3 ($C_{95}H_{140}PO_4^-$; 1376.05 Da). To validate the ability of the methods to resolve Dol-P of varying lengths, a mixed Dol-P standard comprising C_{85} - C_{105}-Dol-P, which are typical for mammalian cells [1], was labelled with 9-ADM and separated by HPLC. A dimethylation and subsequent selective demethylation was included in the Dol-P preparation to improve product stability as established by Yamada *et al.* [15]. The fluorescent profile of monomethylated and 9-ADM labelled mixed Dol-P standard showed a clean separation of C_{85}-Dol-P, C_{90}-Dol-P, C_{95}-Dol-P, C_{100}-Dol-P and C_{105}-Dol-P (Fig. 3A). The ESI-MS analysis of the unlabelled mixed Dol-P standard confirmed the presence of Dol-P species in comparable ratios to those

detected by HPLC (Fig. 3C, i.e. C_{85}-Dol-P at m/z 1257.2, C_{90}-Dol-P at m/z 1325.1, C_{95}-Dol-P at m/z 1393.1, C_{100}-Dol-P at m/z 1461.0, and C_{105}-Dol-P at m/z 1528.9).

To investigate the Dol-P pool of cultured cells, we prepared batches of 2.0 x 10^8 HeLa cells. After purification and separation of Dol-P from polyprenol alcohols, 75% of the samples were labelled with 9-ADM and analyzed by HPLC. The resulting chromatograms showed that Dol-P in HeLa cells mainly consisted of C_{95}-Dol-P (Fig. 3B), which was in agreement with earlier reports on various human tissues [25; 26]. Additionally, C_{90}- and C_{100}-Dol-P were detected, but to a lower extend (Fig. 3B). By contrast, the C_{85}- and the C_{105}-Dol-P species were either completely absent or their amounts were below the detection level.

The remaining 25% of the purified Dol-P pool from HeLa cells were subjected to nano-ESI-MS analysis without further treatment. Again, the main species C_{95}-Dol-P at m/z 1392.7 was flanked by lower amounts of C_{90}-Dol-P at m/z 1324.8 and C_{100}-Dol-P at m/z 1460.8 (Fig. 3D). The enhanced sensitivity of nano-ESI-MS compared to HPLC allowed the detection of minimal amounts of C_{85}- and C_{105}-Dol-P at m/z 1256.3 and 1529.0, respectively. To allow the quantification of Dol-P levels in HeLa cells, 25 µg of C_{80}-polyprenol-P standard were added to each cell samples before extraction. Dol-P and polyprenol-P were separated by HPLC and the corresponding peak areas compared (Fig. 4A). An amount of 1.43 µg Dol-P per 10^8 HeLa cells was calculated, which represented the sum of 0.21 µg of C_{90}-Dol-P, 0.81 µg of C_{95}-Dol-P, 0.40 µg of C_{100}-Dol-P and 0.01 µg of C_{105}-Dol-P (Fig. 4C). The linearity of Dol-P quantification was confirmed by measuring increasing ratios of spiked C_{80}-polyprenol standard to HeLa cell extracts (Fig. 4D).

Dol and cholesterol share the same biosynthetic pathway until the formation of the C_{15}-farnesyl-pyrophosphate intermediate [2]. Hence, statins inhibiting the 3-hydroxy-3-methyl-glutaryl-CoA reductase enzyme do not only act as cholesterol lowering drugs,

but also affect the synthesis of Dol and Dol-P [27; 28]. To investigate the impact of statins on the level and composition of the Dol-P pool of HeLa cells, we added 50 µM pravastatin [29; 30] to the cell culture medium for 72 h. The separation of the resulting 9-ADM labelled Dol-P by HPLC showed an overall reduction of Dol-P, which was more pronounced for Dol-P species of large isoprene chain lengths (Fig. 4B). The pravastatin treatment decreased C_{90}-Dol-P to 0.20 µg per 10^8 HeLa cells, whereas C_{95}-Dol-P was reduced to 0.29 µg per 10^8 cells. Only minor amounts of C_{100}-Dol-P, below 0.01 µg per 10^8 cells were detected (Fig. 4C). The overall levels of Dol-P were reduced to 0.50 µg per 10^8 cells, representing 35% of the normal Dol-P levels in HeLa cells.

Discussion

The present study describes two methodological approaches to analyse and quantify low amounts of Dol-P from cultured human cells. Recording of negative ion ESI-MS spectra allowed us to determine the isoprene chain length and the saturation state of the α-isoprene of mixed polyprenol-P samples. In addition, the separation of 9-ADM labelled Dol-P and polyprenol-P by HPLC enabled the quantitative determination of Dol-P by comparison with known amounts of C_{80}-polyprenol-P internal standard.

The limited sample volume of cultured human cell renders the detection of Dol-P a challenging task. To ensure a reliable measurement, the application of sensitive methods such as ESI-MS and fluorescence detection is indispensable. Along this line, the direct UV-detection of Dol-P established by Elmberger *et al.* [12] is not applicable at the cell culture scale. Earlier approaches also applied metabolic labelling of the polyprenol chain with [^{3}H]-acetic acid or -mevalonate [31; 32] or fluorescent labelling of the phosphate group [15; 33]. The disadvantages of isotopic labelling, such as interference of exogenously added intermediates on Dol biosynthesis or variable incorporation of the isotopes, significantly impair the quantitative determination of Dol-P. The fluorescent labelling of phosphate groups enables both the sensitive detection and the reliable quantitative measurement of Dol-P in cell cultures. In this context, the fluorophore 9-ADM has the advantage of being commercially available in contrast to other compounds applied earlier [15]. However, the drawback of 9-ADM labelling itself was a poor reproducibility because of high susceptibilty to hydrolysis. To increase the stability of the compounds during the labelling procedure, Dol-P samples were first dimethylated and selectively demethylated [15]. This step dramatically improved the stability and reproducibility of the procedure, which once optimized enabled the detection of Dol-P at the ng range (Fig. 4).

In all ESI-MS spectra recorded, additional signals incrementing with 16 Da could be observed. We assume that these signals were generated by oxidation of double bonds within the isoprenes, either by spontaneous epoxidation [34] or by [2 + 2] cycloaddition of molecular oxygen [35]. This phenomenon has already been observed earlier [18] and we found it more pronounced when derivatizing polyprenol-P. Constant sample storage in darkness, at -20°C and under inert atmosphere helped at keeping the oxidation to low levels.

The present combined approach can be used for the analysis of Dol-P in cells under various pathological conditions. Recently, the first inherited human disorder affecting the Dol-kinase and hence Dol-P biosynthesis has been described [10]. Since disrupted Dol phosphorylation has severe implications on protein N-glycosylation, Dol-kinase deficiency is counted as a form Congenital Disorders of Glycosylation (CDG). It is likely that additional genes from the Dol-P biosynthetic pathway, such as the *cis*-prenyltransferase, the polyprenol mono- or pyrophosphatases or the polyprenol-reductase [24] may soon be found as cause of CDG. Accordingly, the present technique represents an ideal screening tool for the detection of truncated or incompletely saturated Dol-P in patient derived fibroblasts.

We did test our Dol-P quantification method by evaluating the effect of the 3-hydroxy-3-methyl-glutaryl-CoA reductase inhibitor pravastatin [29] on Dol-P levels in HeLa cells. The statin leads to a striking decrease of Dol-P levels in addition to its action on cholesterol biosynthesis. The overall reduction to 35% of control levels mostly results from by the loss of large Dol-P species. The reason why large Dol-P are more susceptible to pravastatin treatment is unclear but it is likely that *cis*-prenyltransferase leads to shorter polyprenols species under conditions of limited mevalonate availability. Along this line, part of the numerous side effects of pravastatin [36] could be explained by

inhibition of the diverging isoprenoid pathways leading to the formation of Dol, ubiquinone or prenylated proteins [2]. Low levels of free Dol and Dol-P might lead to eczema, itching and loss of hair, as observed in Dol-kinase deficient patients [10]. Reduced N-linked and O-mannose glycosylations due to limited amounts of the membrane anchor Dol-P might contribute to muscle and liver problems.

In conclusion, the introduced methodology provides a reliable analytical setup to address the impact of drugs and other treatments on Dol-P in cell culture models and to identify novel inherited disorders affecting Dol-P biosynthesis.

Acknowledgements

This work was supported by the Swiss National Science Foundation grant 31003A-116039 to TH.

Abbreviations

9-anthryldiazomethane	=	9-ADM
Dolichol	=	Dol
Dolichol-phosphate	=	Dol-P
Electrospray ionization mass spectrometry	=	ESI-MS
Congenital Disorders of Glycosylation	=	CDG

References

[1]T. Chojnacki, and G. Dallner, The biological role of dolichol. Biochem. J. 251 (1988) 1-9.

[2]E. Swiezewska, and W. Danikiewicz, Polyisoprenoids: structure, biosynthesis and function. Prog. Lipid Res. 44 (2005) 235-58.

[3]B. Schenk, F. Fernandez, and C.J. Waechter, The ins(ide) and out(side) of dolichyl phosphate biosynthesis and recycling in the endoplasmic reticulum. Glycobiology 11 (2001) 61-70.

[4]R. Kornfeld, and S. Kornfeld, Assembly of asparagine-linked oligosaccharides. Annu. Rev. Biochem. 54 (1985) 631-64.

[5]S. Strahl-Bolsinger, M. Gentzsch, and W. Tanner, Protein O-mannosylation. Biochim. Biophys. Acta 1426 (1999) 297-307.

[6]T. Kinoshita, K. Ohishi, and J. Takeda, GPI-anchor synthesis in mammalian cells: genes, their products, and a deficiency. J. Biochem. 122 (1997) 251-7.

[7]I. Eggens, L. Backman, A. Jakobsson, and C. Valtersson, The lipid composition of highly differentiated human hepatomas, with special reference to fatty acids. Br. J. Exp. Pathol. 69 (1988) 671-83.

[8]M. Soderberg, C. Edlund, I. Alafuzoff, K. Kristensson, and G. Dallner, Lipid composition in different regions of the brain in Alzheimer's disease/senile dementia of Alzheimer's type. J. Neurochem. 59 (1992) 1646-53.

[9]N.A. Hall, and A.D. Patrick, Dolichol and phosphorylated dolichol content of tissues in ceroid-lipofuscinosis. J. Inherit. Metab. Dis. 8 (1985) 178-83.

[10]C. Kranz, C. Jungeblut, J. Denecke, A. Erlekotte, C. Sohlbach, V. Debus, H.G. Kehl, E. Harms, A. Reith, S. Reichel, H. Grobe, G. Hammersen, U. Schwarzer, and T.

Marquardt, A defect in dolichol phosphate biosynthesis causes a new inherited disorder with death in early infancy. Am. J. Hum. Genet. 80 (2007) 433-40.

[11]M. Bizri, J.F. Bouhours, Y. Bizri, and R. Got, Separation and quantitative determination of dolichol and dolichyl phosphate in rat and trout liver. Comp. Biochem. Physiol. B 84 (1986) 565-9.

[12]P.G. Elmberger, I. Eggens, and G. Dallner, Conditions for quantitation of dolichyl phosphate, dolichol, ubiquinone and cholesterol by HPLC. Biomed. Chromatogr. 3 (1989) 20-8.

[13]R.K. Keller, J.W. Tamkun, and W.L. Adair, Jr., Development of quantitative assay for tissue levels of dolichyl phosphate. Biochemistry 20 (1981) 5831-6.

[14]N. Chaudhary, D.J. Freeman, J.W. Rip, and K.K. Carroll, Direct estimation of dolichyl phosphate in rat liver by high pressure liquid chromatography. Lipids 17 (1982) 558-60.

[15]K. Yamada, S. Abe, T. Suzuki, K. Katayama, and T. Sato, A high-performance liquid chromatographic method for the determination of dolichyl phosphates in tissues. Anal. Biochem. 156 (1986) 380-5.

[16]K. Skorupinska-Tudek, T. Bienkowski, O. Olszowska, M. Furmanowa, T. Chojnacki, W. Danikiewicz, and E. Swiezewska, Divergent pattern of polyisoprenoid alcohols in the tissues of Coluria geoides: a new electrospray ionization MS approach. Lipids 38 (2003) 981-90.

[17]H. Zhang, K. Ohyama, J. Boudet, Z. Chen, J. Yang, M. Zhang, T. Muranaka, C. Maurel, J.K. Zhu, and Z. Gong, Dolichol biosynthesis and its effects on the unfolded protein response and abiotic stress resistance in Arabidopsis. Plant Cell 20 (2008) 1879-98.

[18]W.J. Griffiths, M. Hjertman, A. Lundsjö, J. Wejde, J. Sjövall, and O. Larsson, Analysis of dolichols and polyprenols and their derivatives by electron impact, fast atom bombardment and electrospray ionization tandem mass spectrometry. Rapid Commun. Mass Spectrom. 10 (1996) 663-75.

[19]W.C. Ward, F.A. Zucca, C. Bellei, L. Zecca, and J.D. Simon, Neuromelanins in various regions of human brain are associated with native and oxidized isoprenoid lipids. Arch. Biochem. Biophys. 484 (2009) 94-9.

[20]T.A. Garrett, Z. Guan, and C.R. Raetz, Analysis of ubiquinones, dolichols, and dolichol diphosphate-oligosaccharides by liquid chromatography-electrospray ionization-mass spectrometry. Methods Enzymol. 432 (2007) 117-43.

[21]F.L. D'Alexandri, F.C. Gozzo, M.N. Eberlin, and A.M. Katzin, Electrospray ionization mass spectrometry analysis of polyisoprenoid alcohols via Li+ cationization. Anal. Biochem. 355 (2006) 189-200.

[22]B.A. Wolucka, and E. de Hoffmann, Mass spectrometric analysis of prenyl phosphates and their glycosylated forms. Acta Biochim. Pol. 41 (1994) 345-9.

[23]T. Imbach, B. Schenk, E. Schollen, P. Burda, A. Stutz, S. Grunewald, N.M. Bailie, M.D. King, J. Jaeken, G. Matthijs, E.G. Berger, M. Aebi, and T. Hennet, Deficiency of dolichol-phosphate-mannose synthase-1 causes congenital disorder of glycosylation type Ie. J. Clin. Invest. 105 (2000) 233-9.

[24]T. Ohkura, K. Fukushima, A. Kurisaki, H. Sagami, K. Ogura, K. Ohno, S. Hara-Kuge, and K. Yamashita, A partial deficiency of dehydrodolichol reduction is a cause of carbohydrate-deficient glycoprotein syndrome type I. J. Biol. Chem. 272 (1997) 6868-75.

[25]M. Andersson, E.L. Appelkvist, K. Kristensson, and G. Dallner, Distribution of dolichol and dolichyl phosphate in human brain. J. Neurochem. 49 (1987) 685-91.

[26]O. Tollbom, and G. Dallner, Dolichol and dolichyl phosphate in human tissues. Br. J. Exp. Pathol. 67 (1986) 757-64.

[27]E.L. Appelkvist, C. Edlund, P. Low, S. Schedin, A. Kalen, and G. Dallner, Effects of inhibitors of hydroxymethylglutaryl coenzyme A reductase on coenzyme Q and dolichol biosynthesis. Clin. Investig. 71 (1993) 97-102.

[28]I.M. Astrand, E. Fries, T. Chojnacki, and G. Dallner, Inhibition of dolichyl phosphate biosynthesis by compactin in cultured rat hepatocytes. Eur. J. Biochem. 155 (1986) 447-52.

[29]T. Koga, Y. Shimada, M. Kuroda, Y. Tsujita, K. Hasegawa, and M. Yamazaki, Tissue-selective inhibition of cholesterol synthesis in vivo by pravastatin sodium, a 3-hydroxy-3-methylglutaryl coenzyme A reductase inhibitor. Biochim. Biophys. Acta 1045 (1990) 115-20.

[30]D. McTavish, and E.M. Sorkin, Pravastatin. A review of its pharmacological properties and therapeutic potential in hypercholesterolaemia. Drugs 42 (1991) 65-89.

[31]T.J. Ekstrom, T. Chojnacki, and G. Dallner, Metabolic labeling of dolichol and dolichyl phosphate in isolate hepatocytes. J. Biol. Chem. 259 (1984) 10460-8.

[32]R.K. Keller, S.W. Nellis, and L. Cuadrado-Simonet, A rapid procedure for the separation and analysis of metabolites of the sterol and dolichol pathways. Chem. Phys. Lipids 51 (1989) 261-7.

[33]L.W. Jiang, B.A. Mitchell, J.G. Teodoro, and J.W. Rip, Uptake and transport of fluorescent derivatives of dolichol in human fibroblasts. Biochim. Biophys. Acta 1147 (1993) 205-13.

[34]V. Gnanadesikan, and E.J. Corey, A strategy for position-selective epoxidation of polyprenols. J. Am. Chem. Soc. 130 (2008) 8089-93.

[35]A.G. Griesbeck, W. Adam, A. Bartoschek, and T.T. El-Idreesy, Photooxygenation of allylic alcohols: kinetic comparison of unfunctionalized alkenes with prenol-type allylic alcohols, ethers and acetates. Photochem. Photobiol. Sci. 2 (2003) 877-81.

[36]D.L. McClure, R.J. Valuck, M. Glanz, and J.E. Hokanson, Systematic review and meta-analysis of clinically relevant adverse events from HMG CoA reductase inhibitor trials worldwide from 1982 to present. Pharmacoepidemiol. Drug Saf. 16 (2007) 132-43.

Figure legends

Figure 1: MS detection of C_{95}-Dol-P and C_{80}-polyprenol-P standards. **(A)** The negative ion MS spectrum of C_{95}-Dol-P shows the expected species with a mass of 1392.17 Da together with small amounts of co-purified C_{90}- and C_{100}-Dol-P. **(B)** The C_{95}-Dol-P at m/z 1392.5 was subjected to collision induced fragmentation and a major fragment ion series started at m/z 164.9 with the $C_5H_{10}PO_4^-$ ion (structure inserted). Further fragments incrementing by 68 Da were detected, consistent with the elimination of single isoprene units from the C_{95}-Dol-P precursor (Table 1). Starting ions of minor fragment series are indicated with an arrow. **(C)** The C_{80}-polyprenol-P standard yielded the expected ion at m/z 1186.7, whereas traces of C_{75}-polyprenol-P and oxidized forms of the hexadecaprenyl-P standard were also detected in the MS spectrum. **(D)** Decay sequences were recorded after the collision induced fragmentation of the main C_{80}-polyprenol-P ion at 1186.7. The primary ion $C_5H_8PO_4^-$ (structure inserted) of the major fragmentation series represents unsaturated monoprenyl-P. The eliminated fragments are identical to those observed for C_{95}-Dol-P in **(B)** (Table 2). The starting ions of minor decay series are indicated with arrows.

Figure 2: HPLC and MS analysis of 9-ADM labelled C_{95}-Dol-P and C_{80}-polyprenol-P standards. **(A)** The 9-ADM labelled C_{95}-Dol-P standard produced a profile with a main peak eluting at 65.1 min and smaller peaks of C_{90}-and C_{100}-Dol-P at 52.8 and 80.7 min. **(B)** The 9-ADM labelled C_{80}-polyprenol-P standard eluted at a retention time of 31.6 min in the HPLC profile. **(C)** The 9-ADM labelled C_{95}-Dol-P peak (structure inserted) was collected from the HPLC run and subjected to MS analysis, yielding a principal ion at m/z 1582.5 and minor ions at m/z 1599.0 and 1615.1, representing oxidation products with the typical 16 Da mass increase. **(D)** The formation of 9-ADM labelled C_{80}-polyprenol-P (structure inserted) was confirmed by MS by detecting a main product at the expected mass at m/z 1376.3.

Figure 3: HPLC and MS analysis of mixed Dol-P standard and Dol-P in HeLa cells. **(A)** A mixed Dol-P standard was monomethylated, labelled with 9-ADM and subsequently separated by HPLC. The distinct Dol-P peaks were identified and marked at the top of the chromatograms. **(B)** The Dol-P pool of HeLa cells was analyzed by HPLC and yielded the main compound C_{95}-Dol-P and smaller amounts of C_{90}- and C_{100}-Dol-P. **(C)** The MS spectrum of unlabelled mixed Dol-P standard confirms the presence of C_{85}-, C_{90}-, C_{95}-, C_{100}- and C_{105}-Dol-P at m/z 1257.2, 1325.1, 1393.1, 1461.0 and 1528.9, respectively. **(D)** The HeLa Dol-P pool yielded an MS profile demonstrating the presence of C_{85}-, C_{90}-, C_{95}-, C_{100}- and C_{105}-Dol-P at m/z 1256.3, 1324.8, 1392.7, 1460.8 and 1529.0, respectively.

Figure 4: Quantification of Dol-P from mock- and pravastatin-treated HeLa cells. **(A)** Dol-P from mock-treated HeLa cells were prepared in presence of 25 µg C_{80}-polyprenol-P as internal standard. Individual Dol-P were assigned in the enlarged section of the profile and quantified by comparison with hexadecaprenyl-P eluting at 34.0 min

(marked by arrow). **(B)** HPLC profile of pravastatin-treated HeLa cells including a C_{80}-polyprenol internal standard (marked by arrow). **(C)** The Dol-P levels from four independent experiments were quantified and normalized to 10^8 HeLa cells. White bars represent Dol-P levels from mock-treated cells and gray bars Dol-P levels from pravastatin-treated cells. Error bars show standard derivations. **(D)** Linear correlation of C_{80}-polyprenol-P standard to HeLa cell extract of four independent experiments against measured Dol-P amounts, linear regression coefficient $R^2 = 0.9943$.

Table 1. Major decay ion series resulting from the fragmentation of C_{95}-Dol-P

Isoprene units	Molecular formula	Theoretical mass [Da]	Detected mass [m/z]
1	$C_5H_{10}PO_4^-$	165.03	164.9
2	$C_{10}H_{18}PO_4^-$	233.09	233.0
3	$C_{15}H_{26}PO_4^-$	301.16	301.1
4	$C_{20}H_{34}PO_4^-$	369.22	369.2
5	$C_{25}H_{42}PO_4^-$	437.28	437.3
6	$C_{30}H_{50}PO_4^-$	505.34	505.5
7	$C_{35}H_{58}PO_4^-$	573.41	573.4
8	$C_{40}H_{66}PO_4^-$	641.47	641.5
9	$C_{45}H_{74}PO_4^-$	709.53	709.3
10	$C_{50}H_{82}PO_4^-$	777.60	777.5
11	$C_{55}H_{90}PO_4^-$	845.66	845.5
19	$C_{95}H_{156}PO_4^-$	1392.17	1392.5

Table 2. Major decay ion series resulting from the fragmentation of C_{80}-polyprenol-P

Isoprene units	Molecular formula	Theoretical mass [Da]	Detected mass [m/z]
1	$C_5H_8PO_4^-$	163.02	162.7
2	$C_{10}H_{16}PO_4^-$	231.08	230.9
3	$C_{15}H_{24}PO_4^-$	299.14	299.0
4	$C_{20}H_{32}PO_4^-$	367.20	367.1
5	$C_{25}H_{40}PO_4^-$	435.27	435.2
6	$C_{30}H_{48}PO_4^-$	503.33	503.3
7	$C_{35}H_{56}PO_4^-$	571.39	571.6
8	$C_{40}H_{64}PO_4^-$	639.45	639.6
9	$C_{45}H_{72}PO_4^-$	707.52	707.5
10	$C_{50}H_{80}PO_4^-$	775.58	775.6
11	$C_{55}H_{88}PO_4^-$	843.64	843.7
16	$C_{80}H_{130}PO_4^-$	1185.97	1186.7

Figure 1

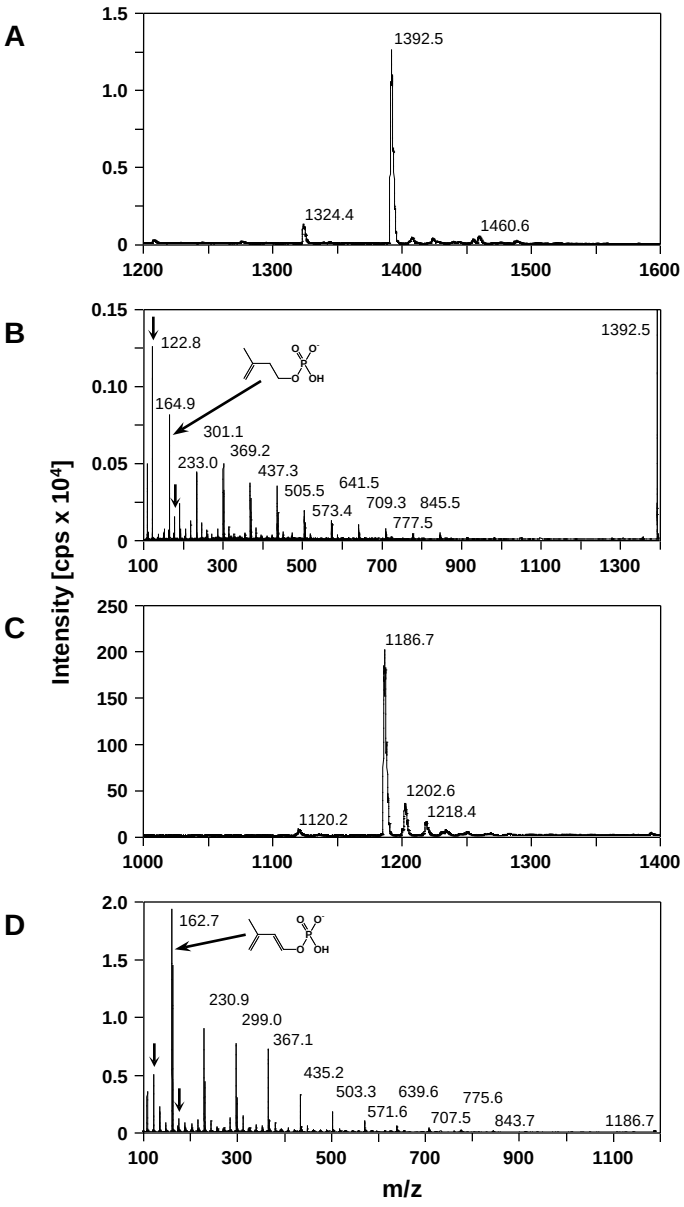
A
1392.5
1324.4
1460.6
B
122.8
164.9
301.1
369.2
233.0
437.3
505.5
641.5
573.4
709.3
845.5
777.5
1392.5
C
1186.7
1202.6
1218.4
1120.2
D
162.7
230.9
299.0
367.1
435.2
503.3
639.6
775.6
571.6
707.5
843.7
1186.7
Intensity [cps x 10⁴]
m/z

Figure 2

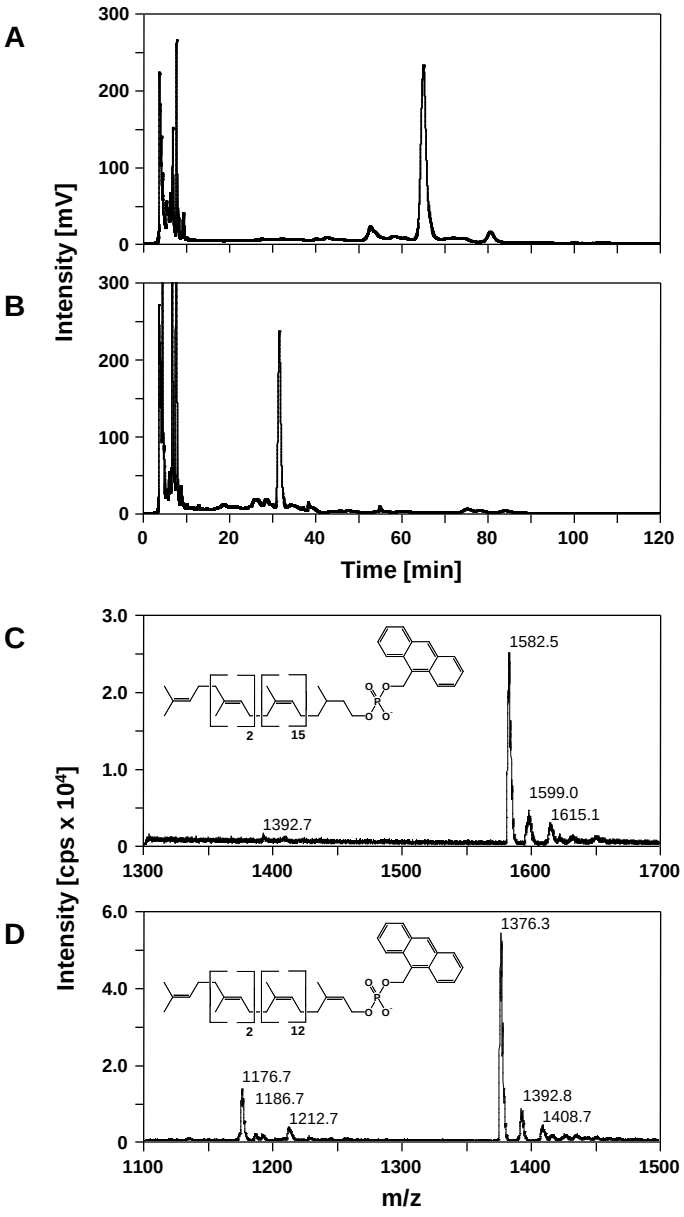
A
B
C
D
Intensity [mV]
Time [min]
Intensity [cps x 10⁴]
m/z
1582.5
1599.0
1615.1
1392.7
1376.3
1392.8
1408.7
1176.7
1186.7
1212.7
2
15
12

Figure 3

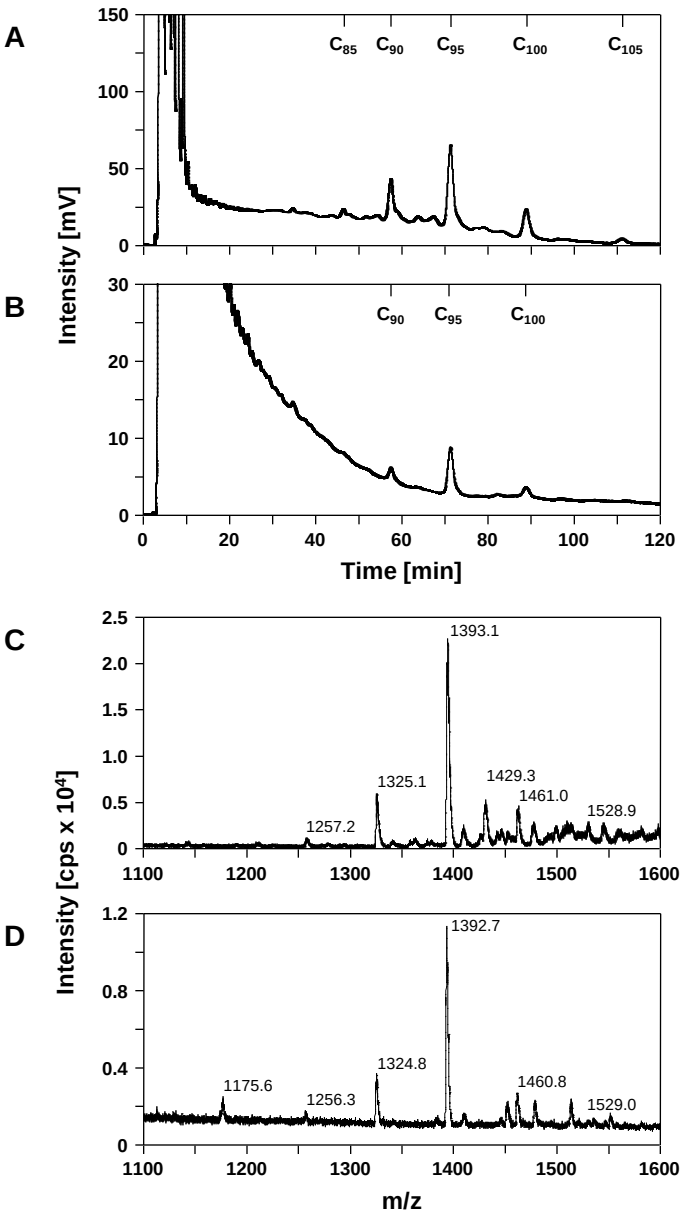
A
B
C
D
Intensity [mV]
Time [min]
Intensity [cps x 10⁴]
m/z
C85 C90 C95 C100 C105
C90 C95 C100
1393.1
1325.1
1429.3
1461.0
1528.9
1257.2
1392.7
1324.8
1460.8
1529.0
1175.6
1256.3

Figure 4

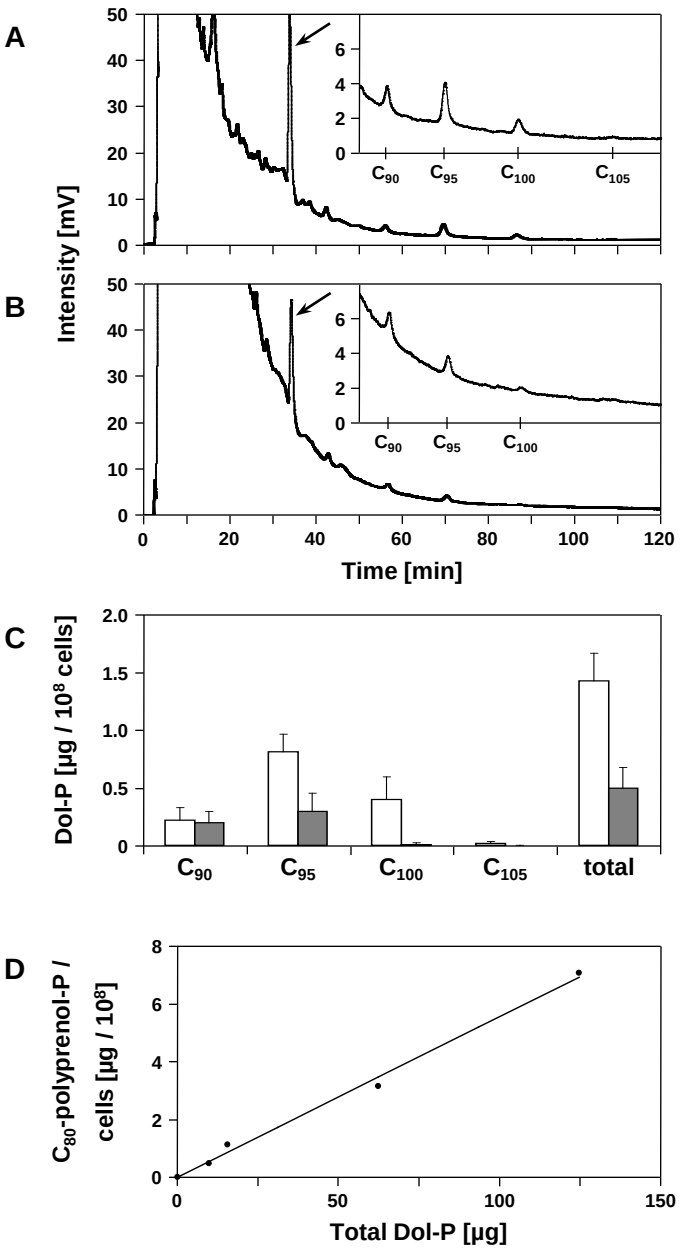
A
B
Intensity [mV]
Time [min]
C
Dol-P [µg / 10^8 cells]
C90
C95
C100
C105
total
D
C80-polyprenol-P / cells [µg / 10^8]
Total Dol-P [µg]